Analyses of Soil-Footing and Soil-Wall Interaction

Analyses d'Interaction de Sol-Semelle et Sol-Mur

T. NAKAI Research Associate, Department of Civil Engineering, Nagoya Institute of Technology, Nagoya, Japan

SYNOPSIS A stress-strain relationship is presented that describes deformation and strength characteristics of soil under the three-dimensional stress condition. Then, finite element analyses for bearing capacity and earth pressure problems are performed by using this relationship. These analytical results by the finite element method explain well various deformation and failure behaviors of soil foundations which have been well-known empirically.

INTRODUCTION

It is one of the most important problems for the finite element analyses of soil foundations to use a stress-strain relationship which expresses soil properties accurately. A stress-strain model has been developed on the basis of "Spatial Mobilized Plane(SMP)" where soil particles are most mobilized on the average under the three-dimensional stress condition(Matsuoka & Nakai, 1974, 1977). In the present paper, a new stress-strain model is proposed by extending the previous model. The model is applied to the finite element analyses of soil-structure interaction problems and the analytical results are compared with those of stability analyses by the theory of plasticity.

STRESS-STRAIN RELATIONSHIP FOR SOIL UNDER THREE-DIMENSIONAL STRESS CONDITION

The total strain increments of soil $\{d\varepsilon\}$ are considered to be expressed as the summation of the plastic strain increments due to shear $\{d\varepsilon^S\}$(the strain increments caused by the change of stress ratio), the plastic strain increments due to consolidation $\{d\varepsilon^C\}$(the strain increments caused by the change of mean principal stress) and the elastic strain increments $\{d\varepsilon^e\}$.

$$\{d\varepsilon\}=\{d\varepsilon^S\}+\{d\varepsilon^C\}+\{d\varepsilon^e\} \qquad (1)$$

Plastic strain increments due to shear $\{d\varepsilon^S\}$

The former stress-strain model has been derived on the idea that unique relationships hold among the shear-normal stress ratio on the SMP(τ_{SMP}/σ_{SMP}) and the normal and shear strain increments on the SMP($d\varepsilon_{SMP}$ and $d\gamma_{SMP}$) (Matsuoka & Nakai, 1974, 1977). Here, new amounts of "strain increments" on the SMP($d\varepsilon^*_{SMP}$ and $d\gamma^*_{SMP}$), which denote the normal and parallel components of the principal strain increment vector to the SMP, are introduced because the average sliding direction of soil particles coincides with the direction of the principal strain increment vector. By using these new amounts $d\varepsilon^*_{SMP}$ and $d\gamma^*_{SMP}$ instead of $d\varepsilon_{SMP}$ and $d\gamma_{SMP}$, a new stress-strain relationship under shear is derived. Now, $d\varepsilon^{*s}_{SMP}$ and $d\gamma^{*s}_{SMP}$ due to shear are given by the following equations in the same manner as the former ones.

$$d\gamma^{*s}_{SMP}=\{\gamma^*_o/(\mu'^*-\mu^*)\}\cdot\exp\{(X-\mu^*)/(\mu'^*-\mu^*)\}\cdot dX \equiv G^*_1\cdot dX \qquad (2)$$

$$d\varepsilon^{*s}_{SMP}=\{(\mu^*-X)/\lambda^*\}\cdot d\gamma^{*s}_{SMP}\equiv E^*_1\cdot dX \qquad (3)$$

where X represents τ_{SMP}/σ_{SMP}, and is given as follows, using the first, second and third effective stress invariants(J_1, J_2 and J_3):

$$X\equiv \tau_{SMP}/\sigma_{SMP}=\sqrt{(J_1\cdot J_2-9J_3)/9J_3} \qquad (4)$$

Of the soil parameters(λ^*, μ^*, μ'^* and γ^*_o) in Eqs.(2) and (3), λ^*, μ^* and μ'^* can be considered to be nearly constant for a given sample. On the other hand, γ^*_o is considered to be a function of mean principal stress σ_m, and is empirically expressed as follows:

$$\gamma^*_o=\gamma^*_{oi}+C^*_d\cdot\log_{10}(\sigma_m/\sigma_{mi}) \qquad (5)$$

If it is assumed that the direction of plastic principal strain increments coincides with that of principal stresses and the direction of $d\gamma^*_{SMP}$ that of the shear stress on the SMP τ_{SMP}, the direction cosines of $d\varepsilon^*_{SMP}$ and $d\gamma^*_{SMP}$ are expressed as follows respectively:

$$a_i=\sqrt{J_3/(\sigma_i\cdot J_2)} \qquad (i=1,\ 2,\ 3) \qquad (6)$$

$$b_i=\{(\sigma_i-\sigma_{SMP})/\tau_{SMP}\}\cdot a_i \quad (i=1,\ 2,\ 3) \quad (7)$$

Accordingly, the principal strain increments $d\varepsilon_i^s$ can be given by the following equations.

$$d\varepsilon_i^s=a_i\cdot d\varepsilon_{SMP}^{*s}+b_i\cdot d\gamma_{SMP}^{*s}$$
$$=(a_i\cdot E_1^*+b_i\cdot G_1^*)\cdot dX$$
$$\equiv A_i\cdot dX \quad (i=1,\ 2,\ 3) \quad (8)$$

or $\{d\varepsilon_i^s\}=\{A_i\}\cdot dX$ (9)

Then, performing the total differentiation of Eq.(4), dX is represented by using the general stress increments $\{d\sigma\}$.

$$dX=\{\partial X/\partial\sigma\}^T\cdot\{d\sigma\}\equiv\{a\}^T\cdot\{d\sigma\} \quad (10)$$

Therefore, the general strain increments due to shear $\{d\varepsilon^s\}$ can be expressed as follows by using the matrix [T] which transforms the principal strain increments $\{d\varepsilon_i^s\}$ into the general strain increments $\{d\varepsilon^s\}$:

$$\{d\varepsilon^s\}=[T]\cdot\{d\varepsilon_i^s\}=[T]\cdot\{A_i\}\cdot\{a\}^T\cdot\{d\sigma\} \quad (11)$$

Plastic strain increments due to consolidation $\{d\varepsilon^c\}$

Upon the consideration about anisotropic consolidation tests, the plastic principal strain increments due to consolidation $d\varepsilon_i^c$ are assumed to be divisible into the components under isotropic consolidation $d\varepsilon_{i(iso)}^c$ and the components due to dilatancy under anisotropic consolidation $d\varepsilon_{i(dil)}^c$. $d\varepsilon_{i(iso)}^c$ are determined from the e-$\log_{10}\sigma_m$ relationship under isotropic consolidation. $d\varepsilon_{i(dil)}^c$ are expressed by the following "strain increments" ($d\varepsilon_{SMP}^{*c}$ and $d\gamma_{SMP}^{*c}$) in the same manner as under shear.

$$d\gamma_{SMP}^{*c}=0.434K_c\cdot[\exp\{(X-\mu^*)/(\mu'^*-\mu^*)\}-\exp\{-\mu^*/(\mu'^*-\mu^*)\}]\cdot(d\sigma_m/\sigma_m)$$
$$\equiv G_2^*\cdot d\sigma_m \quad (12)$$

$$d\varepsilon_{SMP}^{*c}=\{(\mu^*-X)/\lambda^*\}\cdot d\gamma_{SMP}^{*c}\equiv E_2^*\cdot d\sigma_m \quad (13)$$

Accordingly, the principal strain increments $d\varepsilon_i^c$ are given as follows:

$$d\varepsilon_i^c=d\varepsilon_{i(iso)}^c+d\varepsilon_{i(dil)}^c$$
$$=\frac{0.434}{3}\cdot\frac{C_c-C_s}{(1+e_o)}\cdot\frac{d\sigma_m}{\sigma_m}+a_i\cdot d\varepsilon_{SMP}^{*c}+b_i\cdot d\gamma_{SMP}^{*c}$$
$$=(\frac{0.434}{3}\cdot\frac{C_c-C_s}{(1+e_o)\sigma_m}+a_i\cdot E_2^*+b_i\cdot G_2^*)\cdot d\sigma_m$$
$$\equiv B_i\cdot d\sigma_m \quad (i=1,\ 2,\ 3) \quad (14)$$

or $\{d\varepsilon_i^c\}=\{B_i\}\cdot d\sigma_m$ (15)

where C_c is the compression index, C_s the swelling index and e_o the initial void ratio. $d\sigma_m$ is represented as follows by using the general stress increments $\{d\sigma\}$:

$$d\sigma_m=[1/3,\ 1/3,\ 1/3,\ 0,\ 0,\ 0]\cdot\{d\sigma\}\equiv\{b\}^T\cdot\{d\sigma\} \quad (16)$$

Therefore, the general strain increments due to consolidation $\{d\varepsilon^c\}$ can be given in the same manner as $\{d\varepsilon^s\}$ in Eq.(11).

$$\{d\varepsilon^c\}=[T]\cdot\{d\varepsilon_i^c\}=[T]\cdot\{B_i\}\cdot\{b\}^T\cdot\{d\sigma\} \quad (17)$$

Elastic strain increments $\{d\varepsilon^e\}$

The elastic strain increments are given by the incremental stress-strain relationship for an isotropic elastic material.

$$\{d\varepsilon^e\}=[D_e]^{-1}\cdot\{d\sigma\} \quad (18)$$

In Eq.(18), the tangential bulk modulus K_e is determined by the swelling index C_s, and Poisson's ratio ν_e is obtained from the measured unloading stress-strain relationship in a shear test.

By substituting Eqs.(11), (17) and (18) into Eq.(1), a stress-strain relationship in the general coordinate system can be derived. $\{d\varepsilon^s\}$ is considered to be 0 in the case of $dX\leq0$, and $\{d\varepsilon^c\}$ is considered to be 0 in the case of $d\sigma_m\leq0$. By the way, the coefficient K_c in Eq.(12) is determined by using the K_o value and the soil parameters on condition that this relationship satisfies the K_o-consolidation condition.

The failure criterion employed in the finite element analyses is represented by τ_{SMP}/σ_{SMP}= const. or $J_1\cdot J_2/J_3$=const.(Matsuoka & Nakai, 1974, 1977). Fig.1 shows this criterion in terms of the relationship between the internal friction angle ϕ and $b=(\sigma_2-\sigma_3)/(\sigma_1-\sigma_3)$.

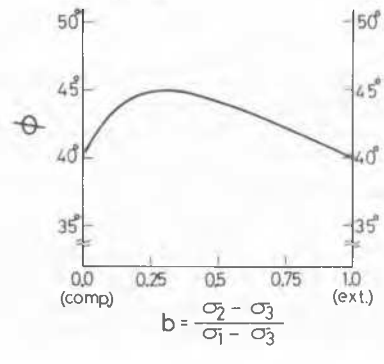

Fig.1 Failure Criterion Based on SMP

It has been proved by true triaxial tests on a sand that this criterion explains well the strength of soil under three principal stresses.

ANALYSES OF SOIL ELEMENT TESTS

The validity of the proposed stress-strain model is discussed here by analyzing various kinds of soil element tests. The soil parameters of the medium dense Toyoura sand(e_o≒0.68) used in the finite element analyses are shown in Table I, which can be determined from constant mean principal stress tests and consolidation tests under triaxial compression. Fig.2 compares the computed stress-strain curves with the measured values by triaxial compression and triaxial extension tests under a constant mean principal stress. Fig.3 shows the comparison of computed values with measured values of triaxial compression and triaxial extension tests under constant principal stress ratios($R \equiv \sigma_1/\sigma_3$) in terms of the volumetric strain ε_v-$\log_{10}\sigma_m$ relationship. It is seen from Fig.3 that the computed results explain well the measured dilatancy behaviors of soil under anisotropic consolidation. Figs.4 and 5 represent the computed results under plane strain condition with respect to the σ_1/σ_3-ε_1-ε_v relationship and the b-σ_1/σ_3 relationship respectively. It is clear from Fig.5 that the analytical results of b are different depending on the stress paths at low stress level, but converge to a certain value between 0.3 and 0.4 as the stress level increases. Such analytical results correspond with the experimental results by Lade and Duncan(1973).

ANALYSES OF SOIL-FOOTING INTERACTION

The finite element analyses are performed for the case that a uniform strip load is imposed on a model foundation under plane strain condition. The loading surface is assumed to be smooth, and the initial stresses in the foundation are calculated as K_o=0.45 and the unit weight γ=15.5kN/m^3. Fig.6 shows the computed distribution of local factors of safety in the foundation at the stage close to failure (loading pressure q=13,034kN/m^2). The factor of safety F.S. is defined as F.S.=$(\tau_{SMP}/\sigma_{SMP})_f/(\tau_{SMP}/\sigma_{SMP})$, where $(\tau_{SMP}/\sigma_{SMP})_f$ represents the shear-normal stress ratio on the SMP at failure. It seems interesting that the zone where local factors of safety are relatively low corresponds to the slip surface obtained by the Terzaghi's bearing capacity theory. Such realistic results are not obtained without consideration of soil dilatancy under both shear and consolidation. On the other hand, the Terzaghi's ultimate bearing loads estimated as ϕ=40° are q_u≒3,500kN/m^2 (with smooth surface) and 7,000kN/m^2(with rough surface). The reason why the computed value exceeds the above ultimate values might be that

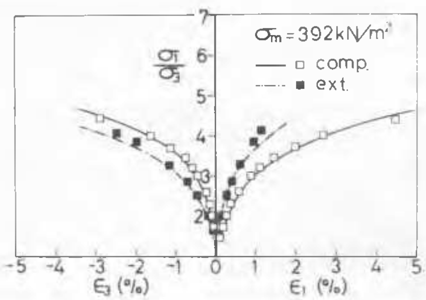

Fig.2 Principal Stress Ratio vs. Principal Strains Relationships by Shear Tests

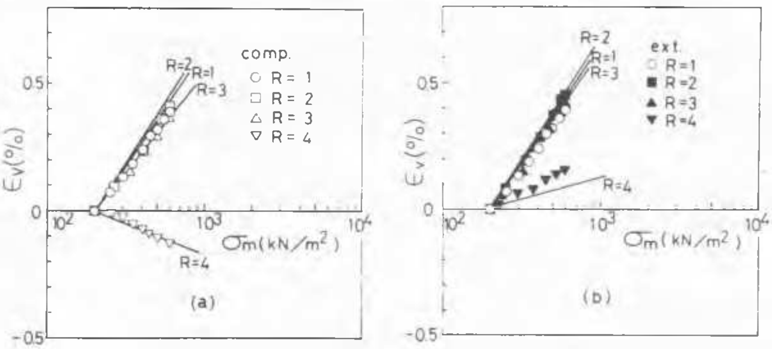

Fig.3 Volumetric Strain vs. Mean Principal Stress Relationships by Consolidation Tests

Table I
Soil Parameters for Toyoura Sand Used in Analyses

λ^*		0.9
μ^*		0.27
μ^{**}		0.41
γ_0^*	γ_{0i}^*	0.10 %
	C_d^*	0.066 %
	σ_{mi}	98 kN/m^2
$C_c/(1+e_0)$		0.928 %
$C_s/(1+e_0)$		0.578 %
K_0		0.45
ν_e		0.3
ϕ (comp)		40°

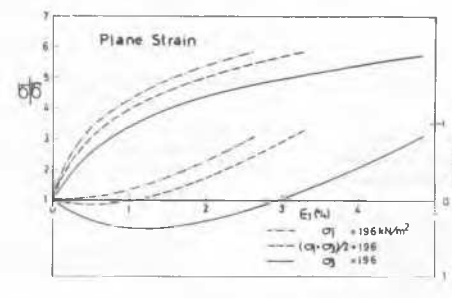

Fig.4 Computed Stress-Strain Curves under Plane Strain Condition

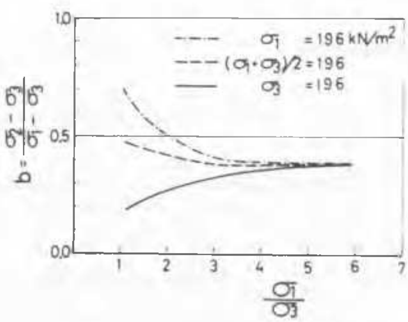

Fig.5 Computed Variations of b-value under Plane Strain Condition

the stress-strain relationship and failure criterion considering the effect of the intermediate principal stress are employed in these analyses.

ANALYSES OF SOIL-RETAINING WALL INTERACTION

Figs.7 and 8 represent the computed distributions of local factors of safety in the backhill behind the retaining wall at the active and passive states respectively. The pattern of wall deflection and the wall displacement d are indicated in each figure. It is seen from these figures that the zones of lower factors of safety are distributed along the slip surfaces, represented by the broken lines, according to the active and passive Coulomb's earth pressure theory. The computed variation of the coefficient of earth pressure K with wall displacement is shown in Fig.9, where the broken lines with dots indicate the values calculated by the Coulomb's theory as ϕ=40°. The computed results show that only little displacement is required to develop the active state, but very large displacement is required to develop the passive state, as has been suggested by many experimental evidences.

CONCLUSIONS

The results may be summarized as follows:

1) The general stress-strain model for soil has been derived by introducing the concept of new amounts of "strain increments" on the SMP($d\varepsilon^*_{SMP}$ and $d\gamma^*_{SMP}$). This model has accounted for deformation and strength characteristics of soil elements under the three-dimensional stress condition.
2) By using this stress-strain model, the finite element analyses have been carried out for the bearing capacity and earth pressure problems. The computed results have explained well various deformation and failure behaviors of soil foundations.

The proposed method of finite element analysis will be also applicable to practical soil engineering problems.

ACKNOWLEDGEMENT

The author wishes to thank Associate Professor H. Matsuoka of Nagoya Institute of Technology for his useful advice and discussion.

REFERENCES

Lade, P.V. & Duncan, J.M.(1973), Cubical triaxial tests on cohesionless soil. Proc. of ASCE, SM10, 793-812.

Matsuoka, H. & Nakai, T.(1974), Stress-deformation and strength characteristics of soil under three different principal stresses. Proc. of Japan Society of Civil Engineers, No.232, 59-70.

Matsuoka, H. & Nakai, T.(1977), Stress-strain relationship of soil based on the "SMP". Proc. of Specialty Session 9, 9th ICSMFE, 153-162.

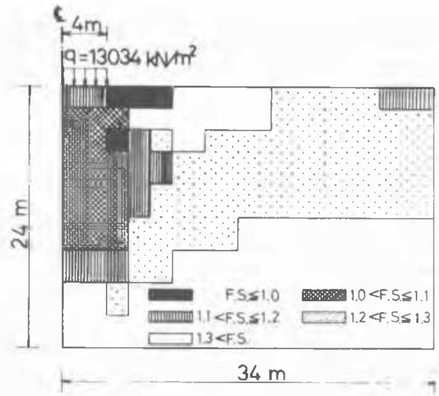

Fig.6 Computed Distribution of Local Factors of Safety under Uniform Strip Load

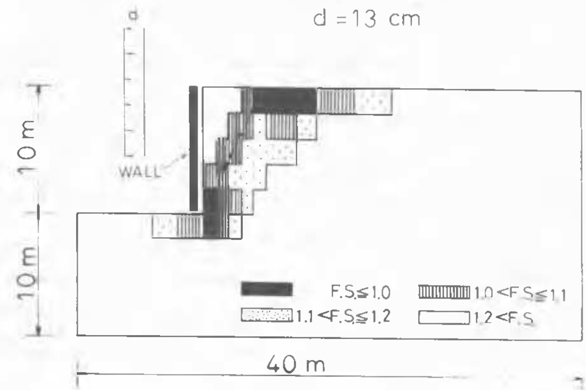

Fig.7 Computed Distribution of Local Factors of Safety at Active Earth Pressure State

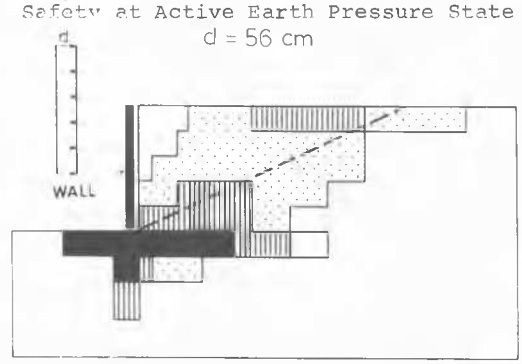

Fig.8 Computed Distribution of Local Factors of Safety at Passive Earth Pressure State

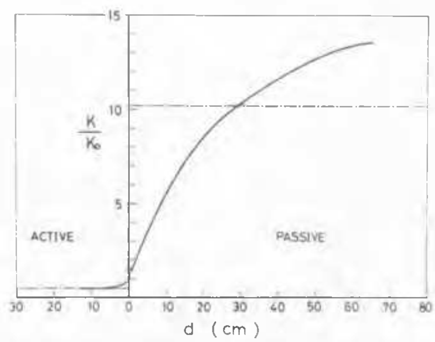

Fig.9 Computed Variation of Earth Pressure Coefficient with Wall Displacement